DP-1479

662742

EVALUATIONS OF THE GENERALIZED AREA AND THE α/υ METHODS OF INTERPRETING PULSED NEUTRON MEASUREMENTS FOR SUBCRITICAL REACTIVITY

P. B. PARKS

E. I. DU PONT DE NEMOURS AND COMPANY
SAVANNAH RIVER LABORATORY
AIKEN, SOUTH CAROLINA 29801

PREPARED FOR THE U.S. DEPARTMENT OF ENERGY UNDER CONTRACT AT(07-2)-1

Printed in the United States of America

Available from
National Technical Information Service
U.S. Department of Commerce
5285 Port Royal Road
Springfield, Virginia 22161

Price: Printed Copy $4.00; Microfiche $3.00

662742

DP-1479

Distribution Category UC-34c

EVALUATIONS OF THE GENERALIZED AREA AND THE α/υ METHODS OF INTERPRETING PULSED NEUTRON MEASUREMENTS FOR SUBCRITICAL REACTIVITY

by

P. B. PARKS

Approved by

J. D. Spencer, Research Manager
Reactor Physics Division

Publication Date: August 1978

E. I. DU PONT DE NEMOURS AND COMPANY
SAVANNAH RIVER LABORATORY
AIKEN, SOUTH CAROLINA 29801

PREPARED FOR THE U. S. DEPARTMENT OF ENERGY UNDER CONTRACT AT(07-2)-1

ABSTRACT

The Generalized Area and α/ν Methods of interpretation of pulsed-neutron measurements for subcritical reactivity were found to minimize the error caused by source-induced harmonics and kinetic distortion. The use of multiple neutron detectors distributed over the core of the reactor in the pulsed source measurements is recommended for increased accuracy of interpretation. The measured data is reduced to a reported value of the subcritical reactivity by the use of numerical solutions to the reactor eigenvalue problems. In the Generalized Area Method, the numerical solution provides an estimate of the static adjoint function which is used to weight the prompt and delayed neutron flux integrals measured in the experiment. These weighted integrals are then used to form the subcritical reactivity. In the α/ν Method, the static eigenequation solved by numerical methods is transformed to a time eigenequation to provide a bridge between the measured decay constant of the fundamental mode and the subcritical static reactivity. Also, the transformation provides a means of normalizing the reported static reactivity.

The evaluations were performed by applying both methods to numerical data generated by one-dimensional, space-time diffusion theory for which k_{eff} was known precisely. The Generalized Area Method was found to deduce reasonably accurate reactivity values from simulations of data from pulsed-neutron experiments in both large and small reflected reactors. The errors from the true reactivity ranged from +3% to -7% in ρ at $k_{eff} = 0.9$. However, the single-detector Sjöstrand analysis failed badly for all pulsing simulations except for that of the small reactor with the source at the center of the core. Errors from the true reactivity ranged from +90% to -260% in ρ at $k_{eff} = 0.9$. The α/ν Method was applicable only to the small-reactor simulation where the error was -1% in ρ at $k_{eff} = 0.9$.

CONTENTS

LIST OF TABLES

LIST OF FIGURES

EVALUATIONS OF THE GENERALIZED AREA AND THE α/ν METHODS OF INTERPRETING PULSED NEUTRON MEASUREMENTS FOR SUBCRITICAL REACTIVITY

INTRODUCTION

The pulsed-source technique has been a standard tool for measuring the subcritical reactivity of shutdown thermal reactors for about twenty years. Numerous experiments have been reported and several schemes have been utilized for the interpretation of the measurements. In recent years, a number of analytical schemes have been proposed. Area Methods proposed by Sjöstrand,[1] Garelis-Russell,[2] and Gozani[3] were introduced in the late 1950's and early 1960's. Preskitt, et al. introduced the Inhour Method,[4] which overcame some of the problems of harmonic and kinetic distortion that badly affected the Area Methods. In recent years, Kosaly, et al.[5] have reinvestigated the original Sjöstrand Method. All of these conventional methods are reviewed in Reference 6.

This report will evaluate two modifications of earlier methods of analysis: the modifications are referred to as the "Generalized Area Method" and the "α/ν Method." In the execution of experiments analyzed by these methods, multiple neutron detectors should be distributed over the subcritical reactor core. Both methods use static reactor codes to reduce the observed pulsed-source responses in the detectors to the subcritical reactivity.

In this discussion, the reactivity sought by both the Generalized Area Method and the α/ν Method is the static reactivity, $\rho_s \equiv (k_{eff_s}^{-1})/k_{eff_s}$. Thus, the results may be compared to a reactivity derived from a static eigenvalue computed by a reactor code. The α/ν Method is shown to be capable of reporting the true static reactivity within the uncertainty of the measurement, but the Generalized Area Method is shown to yield a reactivity which is not the same as the static reactivity (except in special cases). Fortunately, the difference between the Generalized Area reactivity and the static reactivity tends to vanish as the reactivity approaches zero.

The reader is assumed to be familiar with the general description of short-burst neutron experiments as given in several standard texts[7]. Derivations of reactivity expressions for both the Generalized Area and the α/ν Methods will be given. The derivation of the Generalized Area expression is different from that given by Kosály and Fischer,[8] but the results are

essentially the same. Hypothetical pulsing experiments in typical small and large thermal reactors are then modeled with one-dimensional WIGLE calculations[9]. The numerical data from these simulations are then treated by the Generalized Area, the α/ν, and the Sjöstrand methods to determine reactivities. These reactivities are compared to the known reactivity of the simulations to indicate relative accuracies. The sources of error in these methods are also discussed.

GENERALIZED AREA METHOD

A derivation of the Generalized Area Method, given in the Appendix, indicates that

$$\frac{\rho_A}{\beta_{eff_A}} = - \frac{\int_o^{T_o} \int_o^{\infty} \int_o^{Vol} W(\vec{r},E)\ \chi_T(\vec{r},E)\ \overline{P}\ \phi^p(\vec{r},E,t)\ dV\ dE\ dt}{\int_o^{T_o} \int_o^{\infty} \int_o^{Vol} W(\vec{r},E)\ \chi_T(\vec{r},E)\ \overline{P}\ \phi^d(\vec{r},E,t)\ dV\ dE\ dt} \quad (1)$$

where ρ_A = the reactivity (zero at delayed critical) deduced by the Generalized Area approach

β_{eff_A} = the effective delayed-neutron fraction defined in Appendix A

W = unspecified weighting function

$\overline{P}$ = the total neutron production operator

χ_T = the total neutron energy distribution resulting from fission and precursor decay

ϕ^p and ϕ^d = prompt and delayed-neutron fluxes

T_o = the period between repetitive pulses.

The operation of $\overline{P}$ on ϕ is defined as

$$\overline{P}\,\phi \equiv \int_o^{\infty} \nu\Sigma_f\ (\vec{r},E')\phi(\vec{r},E',t)\ dE'.$$

The experiment should be preformed with several neutron detectors distributed over the reactor. The choice of the detector type depends on the reactor type being pulsed. Since $\overline{P}\phi \cong \nu\Sigma_{f_{th}}\ \phi_{th}$ for thermal reactors, a detector of thermal neutrons would be appropriate. Similarly, a fast neutron detector would be appropriate for a fast reactor because $\overline{P}\phi \cong \nu\Sigma_{f_{fast}}\ \phi_{fast}$. The value of $\overline{P}\phi$ will be non-zero only in the core regions of the reactor. Thus, detectors should be placed only in the core.

The only time-dependent quantities in Equation 1 are ϕ^p and ϕ^d. These quantities are not directly measured in pulsed neutron experiments. Usually, counting rates from distributed detectors are stored in the memory of a multiscaler. The prompt counting rate decays rapidly with time after each source burst, and the total counting rate is due only to delayed neutrons at large times within the pulse period. Thus, good estimates of the time integrals of prompt and delayed counting rates are possible. However, the counting rate from neutrons originating from sources other than the pulsed source must first be subtracted over the entire period. Then, the delayed neutron counting rate detected during prompt neutron decay must be estimated and subtracted to form the prompt counting rate. The prompt and delayed counting rate integrals must then be converted to prompt and delayed neutron flux integrals.

Equation 1 may be conveniently approximated from a multigroup perspective. In the two-group diffusion approximation, the Generalized Area reactivity, is given by

$$\frac{\rho_A}{\beta_{eff_A}} \cong - \frac{\sum_{i=1}^{N} \Delta V_i \, W_i^1 \int_o^{T_o} \left(\nu\Sigma_{f_i}^1 \, \phi_i^{p\,1} + \nu\Sigma_{f_i}^2 \, \phi_i^{p\,2} \right) dt}{\sum_{i=1}^{N} \Delta V_i \, W_i^1 \int_o^{T_o} \left(\nu\Sigma_{f_i}^1 \, \phi_i^{d\,1} + \nu\Sigma_{f_i}^2 \, \phi_i^{d\,2} \right) dt} \qquad (2)$$

when using data taken with N neutron detectors. Note that only a fast group weighting function appears in Equation 2 because $\chi_T^2 = 0.0$ in the two-group approximation.

Tests of the Generalized Area Method

The pulsed-neutron experiment has been simulated with numerical computer codes to test the Generalized Area Method equation in two-group form (Equation 2). The simulation is based on the space-time diffusion theory code WIGLE[9] and a corresponding static diffusion theory code. The calculated space-and time-dependent neutron flux responses to a source burst are treated as if they were derived from real experimental data and are analyzed for reactivity by Equation 2.

The static flux and reactivity were calculated in two-energy groups for one-dimensional (slab) hypothetical models. The models reasonably typify small H_2O and large D_2O moderated reactors. The static flux served as the initial flux for a source response calculation with WIGLE. The source was non-zero only for two adjacent mesh points and only in the fast energy group. The neutron-

source duration was fixed at 500 microseconds for all calculations. The WIGLE calculation of the single-burst response was continued for 100 seconds for all pulsing simulations.

The usual pulsed-neutron experiment consists of a measurement of the flux response to a series of periodic source bursts after delayed-neutron equilibrium has been established. The channels of a multi-scaler are turned on sequentially following each source burst; all channels are opened and closed before the next source burst. In a single sweep of the multi-scaler channels at delayed equilibrium, one prompt-neutron response is recorded; however, the delayed-neutron tails from many previous bursts as well as the present burst are also recorded. The single-burst WIGLE response was used to construct the delayed equilibrium response by adding the responses of many identical bursts (each displaced one pulse period from the preceding burst).

Prompt- and delayed-neutron flux integrals of the form $\int_0^{T_0}\phi^P(\vec{r},E,t)\,dt$ and $\int_0^{T_0}\phi^d(\vec{r},E,t)\,dt$ were then formed from the multi-scaler simulations of detector responses at selected positions in the reactor core. The integrals were formed by the technique discussed in the previous section. These integrals were used to compute reactivity by Equation 2.

Two very different thermal reactors were chosen to provide examples of pulsed data. The first, a small H_2O-moderated core (20 cm thick) was surrounded by a H_2O reflector (10 cm on each side). The second, a large D_2O-moderated core (480 cm thick) was surrounded by a D_2O reflector (60 cm on each side). The two-group cross sections and inverse velocities for both reactors are listed in Table 1. The listed $\nu\Sigma_f$ cross sections have been adjusted to produce $k_{eff} = 0.9$ (computed by the static code). The fast group inverse velocity was set equal to zero in every case to facilitate WIGLE convergence.

TABLE 1

Two-Group Cross Sections for Reactor Models

Case	*Reactor*	*D, cm*	Σ_a, *cm*$^{-1}$	Σ_f, *cm*$^{-1}$	$\nu\Sigma_f$, *cm*$^{-1}$	$\Sigma_s^{1\to2}$, *cm*$^{-1}$	χ_T	*1/v, sec/cm*
1	Small H_2O							
	Uniform Core	1.0	8.0×10^{-3}	4.0×10^{-3}	7.6104×10^{-3}	2.0×10^{-2}	1.0	0.0
		0.2	5.0×10^{-2}	1.0×10^{-1}	2.2831×10^{-1}		0.0	3.0×10^{-6}
	Reflector	1.3	5.0×10^{-4}	0.0	0.0	5.0×10^{-2}	0.0	0.0
		0.1	2.0×10^{-2}	0.0	0.0		0.0	4.0×10^{-6}
2	Large D_2O							
	Uniform Core	1.4	1.6×10^{-3}	9.3×10^{-4}	2.0883×10^{-3}	8.2×10^{-3}	1.0	0.0
		0.9	1.3×10^{-2}	9.5×10^{-3}	2.0883×10^{-2}		0.0	3.1×10^{-6}
	Reflector	1.3	1.4×10^{-6}	0.0	0.0	1.2×10^{-2}	0.0	0.0
		0.8	7.5×10^{-5}	0.0	0.0		0.0	4.2×10^{-6}

A common set of β_i and λ_i; values for six families was chosen ($\beta_T = \beta_{eff} = 0.007705$) for convenience. The λ_i, decay constant, values were typical of a H_2O-moderated reactor. Actually, values with much longer-lived photoneutrons should have been chosen for the D_2O-moderated and reflected reactor. This was not done because a longer WIGLE calculation would be required to ensure delayed-neutron equilibrium in the pulsing simulation.

Two sets of WIGLE computations were made for each reactor type. In the first set, the source was placed in the reactor center. In the second set, the source was placed at the core-reflector interface. Two different weighting functions were chosen for this study. The first used a weight of unity everywhere. The second used the static adjoint flux.

Eleven "detectors" were distributed over the core of the small H_2O reactor. Seventeen "detectors" were distributed over the core of the large D_2O reactor. The volume increments represented by each detector were uniform. Table 2 lists the values of the Generalized Area k_{eff} for the two reactor cases. These values were derived from the simulated fluxes at the detector locations for the two different source locations and the two weighting functions. In general, the error with static adjoint weighting was always less than ±1% in k_{eff} at $k_{eff} = 0.9$. For the small core, no accuracy was lost by using uniform weighting. However, uniform weighting of the results in the large core led to a somewhat larger error (-2.9% in k_{eff} at $k_{eff} = 0.9$) when the source was placed at the core edge.

TABLE 2

Generalized Area Multiplication Constants[a]

	Source in Middle		*Source at Core Edge*	
Reactor Type	$W = 1$	$W = \phi_s^+$	$W = 1$	$W = \phi_s^+$
Small H_2O	.8984	.8973	.9014	.9030
Large D_2O	.8968	.8930	.8713	.8928

a. The true static k_{eff} = .9000 in every case.

Comparison of the Generalized Area and Sjöstrand Method Results

Appendix A shows the Generalized Area Method equation (Equation I) takes on the very simple Sjöstrand form if $\psi^p/\psi^d = 1.0$ for all space and time where ψ^p and ψ^d are the shape functions

of the prompt and delayed neutrons (defined in Appendix A). In that case, Equation 1 reduces to

$$-\frac{\rho_{Sjö}}{\beta_{eff_{Sjö}}} = \frac{\int_o^{T_o} \phi^p \, dt}{\int_o^{T_o} \phi^d \, dt} \tag{3}$$

Figure 1 shows the Sjöstrand reactivities for each separately analyzed detector.

The errors of the Sjöstrand Method are due to prompt and delayed harmonic distortions and kinetic distortion. Figures 2-5 show the flux-shape distortion away from the static shapes at selected times for all the pulsing simulations. In these figures, the ratio

$$\frac{\phi(x)/\phi(s)\,|\text{time}}{\phi(x)/\phi(s)\,|\text{static}}$$

is defined as a measure of the distortion where $\phi(x)$ is the time dependent or static flux at position x and $\phi(s)$ is the time dependent or static flux at the source position. A spatially constant flux ratio of 1.0 indicates no distortion.

A derivation of the harmonic shape eigenequations for both prompt and delayed neutrons is given in Appendix C. These derivations indicate that most of the distortion that exists near the peak of the prompt response is from prompt harmonics induced by the source because the first time derivative of the flux is very small, precluding kinetic distortion. After the delayed flux becomes the dominant portion of the flux, most of the distortion is due to delayed harmonics because the first time derivative is again very small. However, during prompt fundamental decay, no prompt harmonic distortion exists, by definition; thus only kinetic distortion may exist whenever the prompt decay is in the fundamental mode.

The delayed harmonic distortion is small for the small H_2O reactor, but the prompt harmonic and kinetic distortions are considerably larger (Figures 2 and 3). In the large D_2O reactor, all the distortions are very severe (Figures 4 and 5). The prompt harmonic distortions were so large for both source positions that a fundamental mode of prompt-neutron decay was not clearly definable.

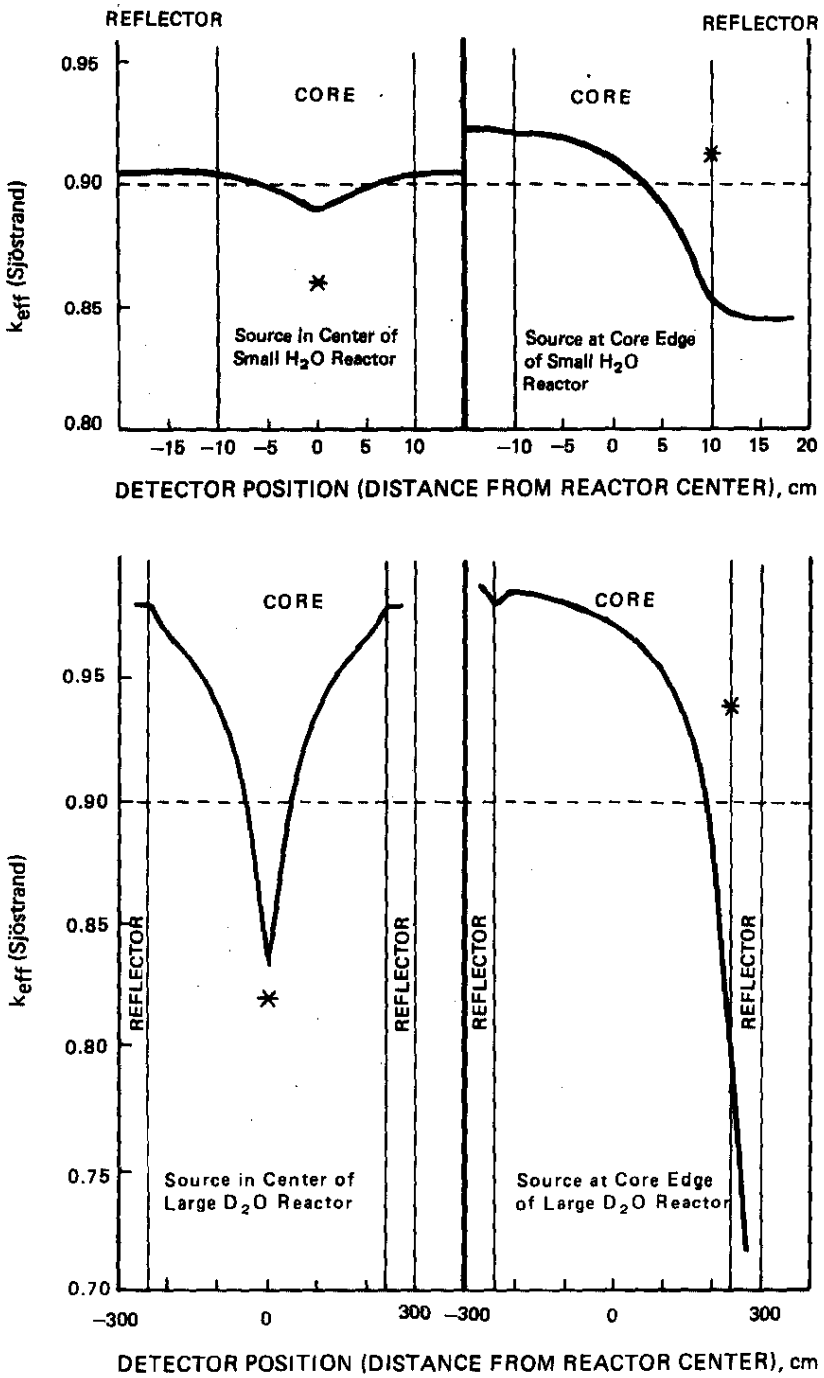

FIGURE 1. K_{eff} from Single-Detector Sjöstrand Analysis. True Static k_{eff} = 0.9

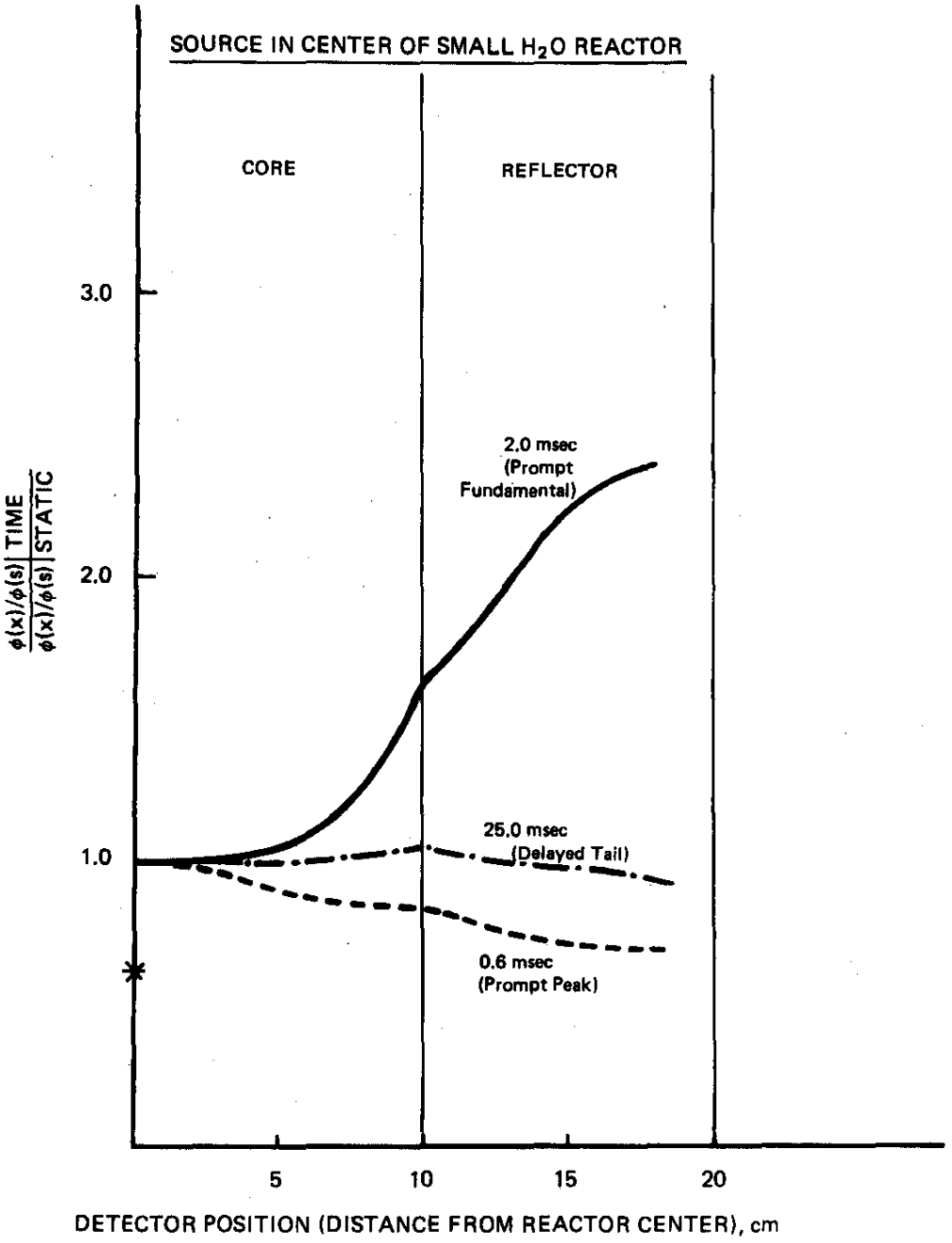

FIGURE 2. Flux-Shape Distortions in Small H_2O Reactor When Pulsed in Center

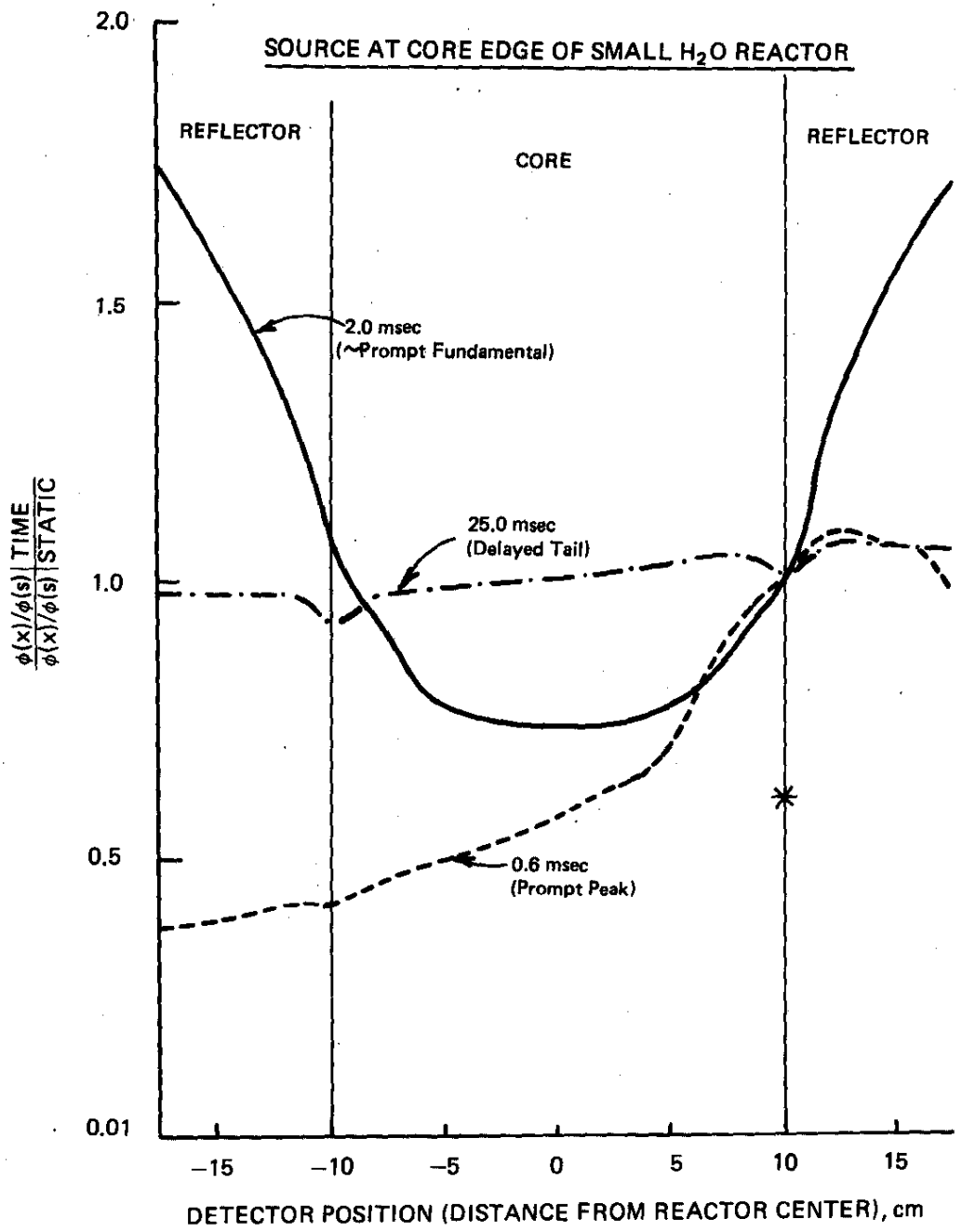

FIGURE 3. Flux-Shape Distortions in Small H_2O Reactor When Pulsed at Core-Reflector Interface

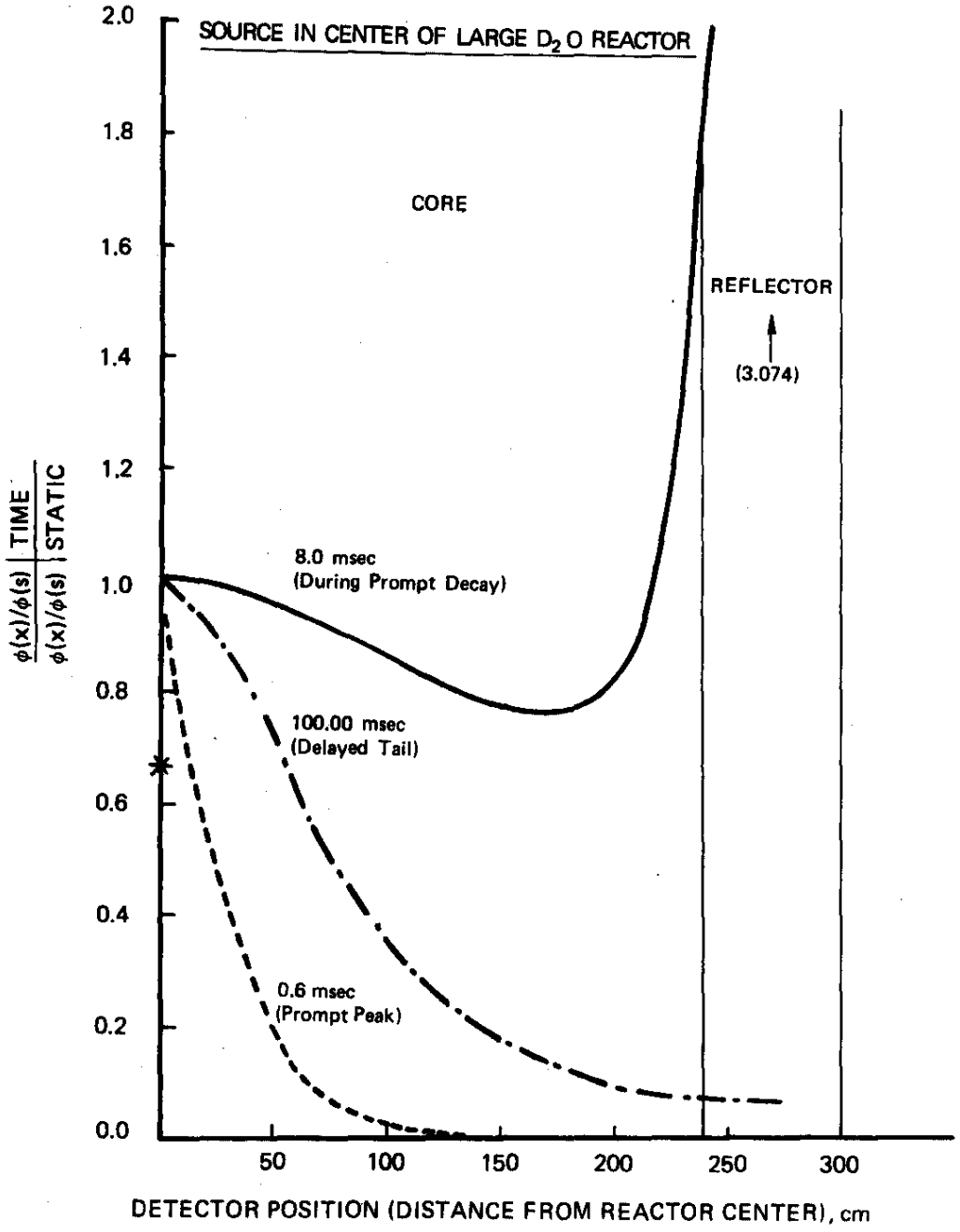

FIGURE 4. Flux-Shape Distortions in Large D_2O Reactor When Pulsed in Center

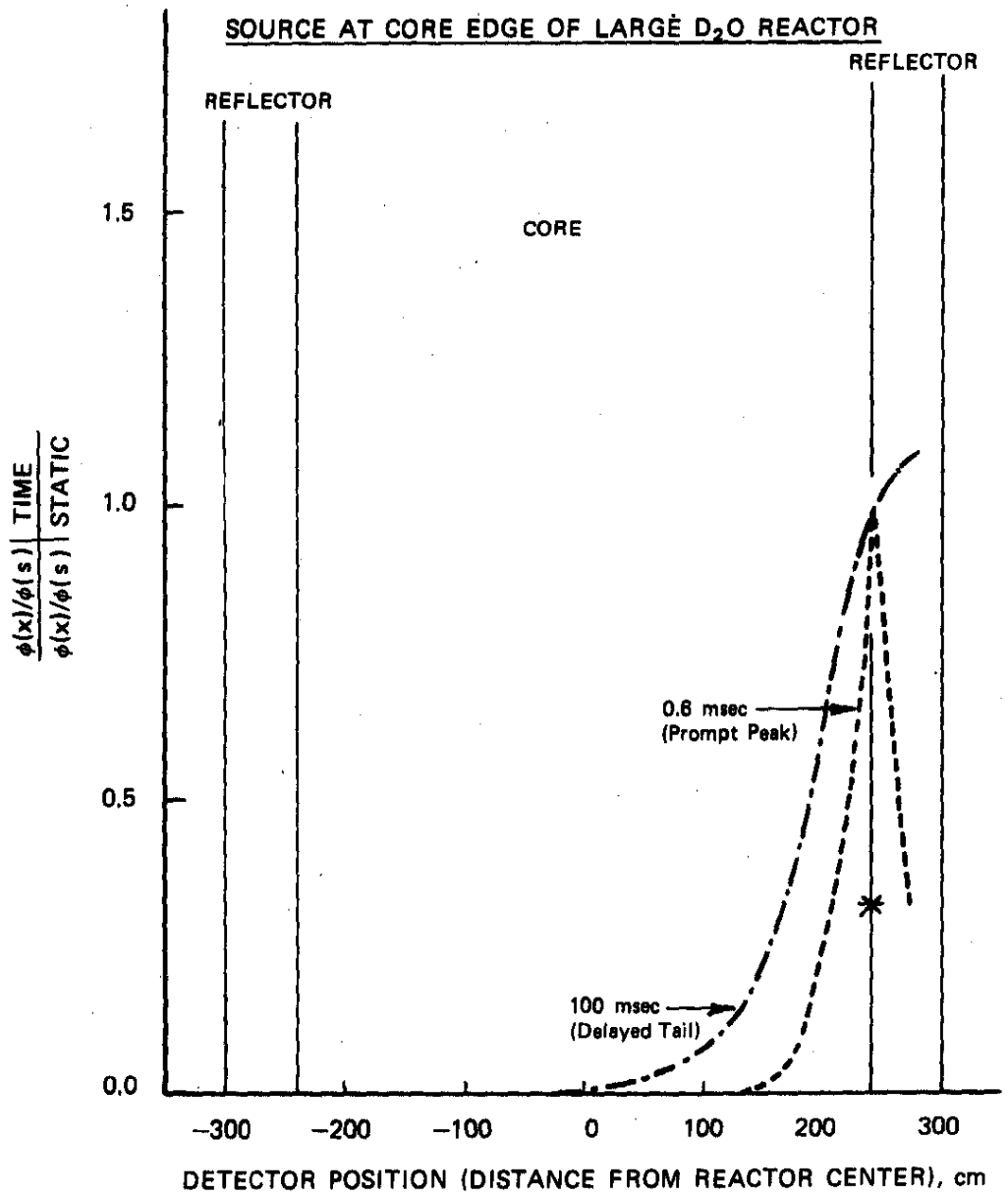

FIGURE 5. Flux-Shape Distortions in Large D_2O Reactor When Pulsed at Core-Reflector Interface

The error of the Sjöstrand Method has been somewhat exaggerated in these simulations by the point description of the fast group external source. In reality, most pulsed sources use the $^3H(d,n)^4He$ reaction which releases neutrons at 14 MeV. As the source neutrons slow down to the average fast group energy, they will spread toward a less strongly peaked distribution than the point distribution used in the WIGLE response calculations. Nevertheless, the errors of the Sjöstrand Method in real, large reactor experiments will be much larger than those of the Generalized Area Method.

Sources of Error in the Generalized Area Method

The reactivity is approximated by Equation 2 in the multi-group form with the assumption that information about ϕP and ϕ^d is obtained only from the multiple neutron detectors. Clearly an integration approximation error exists which can be made acceptably small only by using a relatively large number of detectors.

It is also doubtful that ρ_A/β_{eff_A} is equivalent to the static dollars reactivity ρ_s/β_s, even in the absence of any integration error. This is shown by the following arguments. In the Appendix, the Generalized Area reactivity is defined as

$$\rho_A \equiv \frac{\langle W, [\chi_T \overline{P} - \overline{D}\ ]\ \psi^d \rangle}{\langle W,\ \chi_T \overline{P}\ \psi^d \rangle} = \frac{\langle \phi_s^+,\ [\chi_T \overline{P} - \overline{D}\ ]\ \psi^d \rangle}{\langle \phi_s^+,\ \chi_T \overline{P}\ \psi^d \rangle} \qquad (4)$$

if the code calculated ϕ_s^+ is chosen as the weighting function. $\overline{D}$ is the loss (or destruction) operation which is defined in the Appendix. The neutron flux shape (ψ^d) may be distorted considerably from the fundamental mode flux shape. We define

$$\psi^d = \psi_f^d + \delta\psi^d \qquad (5)$$

where ψ_f^d represents the fundamental mode flux shape of delayed neutrons and $\delta\psi^d$ represents the distortion from the fundamental shape. The Appendix shows that the fundamental mode of ψ^d has very closely the same shape as ϕ_s, the static flux shape calculated by a static code. Thus, the harmonic distorted, delayed flux shape may also be expressed as

$$\psi^d = \phi_s + \delta\psi^d \qquad (6)$$

Therefore

$$\rho_A = \frac{\langle \phi_s^+,\ [\chi_T\ \overline{P} - \overline{D}]\ \phi_s \rangle + \langle \phi_s^+,\ [\chi_T\ \overline{P} - \overline{D}]\ \delta\psi^d \rangle}{\langle \phi_s^+,\ \chi_T\ \overline{P}\ \phi_s \rangle + \langle \phi_s^+,\ \chi_T\ \overline{P}\ \delta\psi^d \rangle} \tag{7}$$

Henry has shown that the static reactivity determined by a code is consistent with

$$\rho_s = \frac{\langle \phi_{s_o}^+,\ [\chi_T\ \overline{P} - \overline{D}]\ \phi_s \rangle}{\langle \phi_{s_o}^+,\ \chi_T\ \overline{P}\ \phi_s \rangle} \tag{8}$$

where $\phi_{s_o}^+$ is the adjoint of the critical ($\rho_s = 0$) flux.[10] If no distortion were present in the delayed neutron flux shape ($\delta\psi^d = 0$), then

$$\rho_A\ (\delta\psi^d=0) = \frac{\langle \phi_s^+,\ [\chi_T\ \overline{P} - \overline{D}]\ \phi_s \rangle}{\langle \phi_s^+,\ \chi_T\ \overline{P}\ \phi_s \rangle} \tag{9}$$

Thus, to the extent that ϕ_s^+ approximates $\phi_{s_o}^+$, $\rho_A\ (\delta\psi^d=0) \cong \rho_s$. However, error terms involving $\delta\psi^d$ will be present in ρ_A whenever significant delayed neutron harmonic distortion exists. Thus, by this analysis, it appears that $\rho_A \neq \rho_s$ when significant harmonic distortion exists in the delayed neutron flux shape. In the small reactor case, $\psi^d \cong \phi^s$ (Figures 2 and 3), and this source of error is small. However, in the large core case, ψ^d is strongly distorted (Figures 4 and 5), and this source of error is not inconsequential.

Similar arguments could be invoked to examine β_{eff_A}. Thus, when one identifies ρ_A/β_{eff_A} as ρ_s/β_{eff_s}, another indeterminant error, in addition to the integration error, is made. The differences of the k_{eff} values reported by the Generalized Area Method (Table 2) from k_{eff_s} equal 0.9 are due to these two sources.

THE α/ν METHOD

The α/ν Method is a modification of Preskitt's Inhour Method.[4] Both methods take advantage of the fact that for a large class of reactors a fundamental mode of decay, α_m, ultimately will be established throughout the reactor following injection of a burst of

neutrons from an extraneous source. This is usually true for thermal reactors, although there are cases for fast reactors where a "quasi-equilibrium" spectrum may not be established and no unique persisting exponential decay may exist.[11] There also may be experimental difficulties in determining α_m. In principle, a single detector could be used to determine α_m. Since the fundamental mode exists only when α can be shown to have approximately the same value at all points in the reactor, the use of multiple detectors is recommended to prove that the decay constant measured is indeed α_m.

In Preskitt's original introduction of the Inhour Method, the static reactivity was shown to be

$$\rho_s = \alpha_m \Lambda_o + \beta_{eff_o} \tag{10}$$

where Λ_o (generation time of the prompt neutron persisting mode) was to be computed with the assistance of a static reactor code. In the α/ν method, a specific calculation of Λ_o is not necessary because a static reactor code can easily be altered to provide a solution to the prompt-neutron eigenequation.

The static k_{eff_s} calculated by a code is the eigenvalue of the static eigenequation which may be expressed as

$$0 = \left[- \overline{D} + k_{eff_s}^{-1} \chi_T \overline{P} \right] \phi_s. \tag{11}$$

For subcritical systems, the calculated eigenvalue, k_{eff_s}, is just the uniform adjustment of $\overline{P}$ necessary to force the right side to zero. The same code is used to solve the prompt neutron eigenequation. This may be done if the following transformations are used:

$\overline{D} + \alpha/\nu$ replaces $\overline{D}$

$(1-\beta_T)\ \overline{P}$ replaces $\overline{P}$

k_p replaces k_{eff}

and χ_p replaces χ_T

$\overline{D}$, $\overline{P}$, and χ_T are transformed by changing the input cross sections of the reactor problem. The transformed eigenequation solved by the reactor code is

$$\left[(- \alpha/\nu - \overline{D}) + k_p^{-1} (1-\beta_T) \chi_p \overline{P} \right] \psi_o^p = 0 \tag{12}$$

where k_p is a scale factor which forces neutron balance; ψ_o^p is the shape function of the fundamental mode of the prompt-neutron distribution; and χ_p is the prompt-neutron energy distribution from fission. Since α_m is a measured quantity, the eigenvalue of the problem is k_p. Though Equation 12 is derived in numerous sources,[4] it is derived in the Appendix C for the sake of completeness.

If the material properties of the reactor were precisely known, the cross sections of all materials were free of error, the geometrical representation were exact, and no solution approximations were made, k_p would always be computed as exactly unity (assuming that α_m was precisely measured). In practice, k_p will usually deviate slightly from unity because the above conditions generally are not precisely met. The effective multiplication constant determined by the experiment is then

$$k_{eff_s}\ (exp) = \frac{k_{eff_s}}{k_p} \tag{13}$$

where k_{eff_s} is the eigenvalue of the untransformed static solution. The corresponding static reactivity determined by the measurement is found from

$$\rho_s\ (exp) = \frac{k_{eff_s}\ (exp) - 1}{k_{eff_s}\ (exp)} \tag{14}$$

However, α_m cannot be determined without error. The errors due to statistical variation of the decaying counting rates may be quantitatively estimated; but an absence of bias from failure to completely establish a fundamental mode without any higher order harmonic contamination is difficult to prove.

Tests of the α/ν Method

The same data developed for the tests of the Generalized Area Method were used for tests of the α/ν Method. The delayed-neutron tails were subtracted from the delayed equilibrium response constructed from the WIGLE calculation. A persisting prompt-neutron decay constant (identified as the fundamental mode decay constant) was determined from the resulting prompt-neutron decay. For the small H_2O-moderated and reflected reactor, the fundamental decay constant appeared to be $-3500 \pm 80\ sec^{-1}$. The uncertainty in α_m was related primarily to the different prompt-neutron harmonic distortions associated with the two-source positions. When the

cross sections (Table 1) were altered by the transformations of the α/ν Method, the eigenvalue of the prompt-neutron eigenequation (k_p) was 1.001. Therefore, k_{eff_s} (exp) = 0.8991. The source of the deviation from the true static reactivity (0.9000) is the uncertainty in α_m.

A fundamental-mode decay constant, reasonably independent of both source and detector positions, could not be defined cleanly from the simulated data for the large D_2O-moderated and reflected reactor. The reason is that the harmonic distortion was very severe due to the very loose coupling of this hypothetical reactor. The prompt harmonics had not died away before the delayed neutrons became the dominant portion of the total flux. Ultimately, a spatially independent decay mode for the prompt neutrons would have been established and observed if delayed neutrons had been removed from the mockup calculations. This mockup is similar to, but larger than, the loosely coupled, D_2O moderated and reflected reactors at the Savannah River Plant. Pulsing measurements on a shutdown SRP reactor mockup were performed recently and the fundamental mode decay constant could not be identified experimentally for the above reasons. However, three-dimensional, pulsed source response calculations without delayed neutrons show that the prompt-neutron decay eventually becomes a fundamental mode decay.

CONCLUSIONS

The Generalized Area Method is successful due to the use of data from multiple neutron detectors and, to a lesser extent, the use of static adjoint weighting of that data. Unit weighting of the data causes somewhat larger inaccuracies for large reactors. The Generalized Area Method copes with difficulties introduced by both harmonic and kinetic distortion of the pulsed source response, whereas the Sjöstrand Method is incapable of accounting for these distortions.

The α/ν Method was more accurate (where applicable) than the Generalized Area Method. To apply the α/ν Method, the decay constant of the fundamental mode must be determined accurately. This task was possible with the small-reactor simulated data, but was impossible for the large-reactor simulated data.

When a fundamental-mode decay can be identified accurately, the α/ν Method should be the preferred method of analysis. One can examine closely the data from multiple detectors and determine a reasonable upper bound on the remaining bias in any α_m measurement caused by higher order harmonics. Alternatively, the Generalized Area Method suffers from an error in approximating certain integrals by discrete sums, an error which is difficult to quantify. Another

error arises from trying to equate ρ_A/β_{eff_A} (defined by the Generalized Area Method) with ρ_s/β_{eff_s} (the static dollar reactivity). This latter error is proportional to the amount of delayed-neutron harmonic distortion.

The α/ν method is preferred, but some situations warrant the use of the Generalized Area Method. There are many situations where numerical solutions of the eigenvalue equation are not possible. Field situations often involve complex geometries beyond the scope of reactor codes or involve unknown material compositions. Also, a clean measurement of the fundamental decay may not be possible, as shown in the pulsing simulations for the large, loosely coupled reactor. For these cases, only the Generalized Area Method with unit weighting is recommended as a simple, yet accurate way of deducing the subcritical reactivity.

If geometric and material modeling is possible, but α_m is not determined, the Space-Time Method may yield a more accurate assessment of the subcritical reactivity than is possible with the Generalized Area Method. However, a large computational effort is required to implement the Space-Time Method. This additional effort is warranted only if the increased accuracy of the Space-Time Method is necessary.

ACKNOWLEDGMENTS

The author wishes to express his thanks to the following individuals: M. Raney for writing the data-handling code by which the pulsed-source response at delayed equilibrium was constructed from the WIGLE single-burst response; J. W. Stewart for adding the time-dependent external source option to WIGLE; C. E. Ahlfeld, W. G. Winn, W. E. Graves, and F. J. McCrosson, Jr. for critical reviews of the report and for many helpful suggestions.

APPENDICES

A. Derivation of the Generalized Area Method Equation

Equation 1 is derived by first breaking up the continuous-energy diffusion equations into separate equations describing the behavior of prompt- and delayed-neutron fluxes. Henry's concepts of the time dependent shape function and amplitude function are introduced along with the time independent weighting function.[10] The special properties of these functions allow one to derive "point reactor" kinetics equations for prompt and delayed neutron amplitude functions. These equations may then be integrated over one pulse period and the Generalized Area Method equation is obtained.

The continuous energy diffusion equations in the stationary fuel form are

$$\frac{1}{v(E)} \frac{\partial \phi(\vec{r},E,t)}{\partial t} = (1-\beta_T(\vec{r})\ \chi_p(\vec{r},E)\ \overline{P}-\overline{D}\ \phi(\vec{r},E,t) + \sum_{i=1}^{M} \chi_i(\vec{r},E)\ \lambda_i(\vec{r},E)\ C_i(\vec{r},t) + S(\vec{r},E,t) \quad \text{(A1)}$$

$$\frac{\partial C_i(\vec{r},t)}{\partial t} = \beta_i(\vec{r})\ \overline{P}\ \phi(\vec{r},E,t) - \lambda_i(\vec{r})\ C_i(\vec{r},t) \quad \text{(A2)}$$

where $\phi(\vec{r},E,t)$ = scalar flux density (or simply flux)

$v(E)$ = neutron speed

$\beta_T(\vec{r})$ = total delayed fraction

$\chi_p(\vec{r},E)$ = prompt energy distribution from fission

$\overline{P}$ = production operator

$\overline{D}$ = loss operator

$\chi_i(\vec{r},E)$ = i'th family delayed neutron energy distribution

$\beta_i(\vec{r})$ = i'th family delayed neutron fraction

$\lambda_i(\vec{r})$ = i'th family decay constant

$C_i(\vec{r},t)$ = i'th family precursor concentration

and $S(\vec{r},E,t)$ = rate of change of neutron density from the pulsed source

The production and loss operators are defined in diffusion theory for pulsed source problems through their operation on ϕ by

$$\overline{P}\,\phi \equiv \int_o^\infty \nu(\vec{r},E')\,\Sigma_f(\vec{r},E')\,\phi(\vec{r},E',t)\,dE' \tag{A3}$$

$$\text{and } \overline{D}\,\phi \equiv \Sigma_t(\vec{r},E)\,\phi(\vec{r},E,t) - \int_o^\infty \Sigma_s(\vec{r},E'\to E)\,\phi(\vec{r},E',t)\,dE' + \nabla\cdot D(\vec{r},E)\,\nabla\phi(\vec{r},E,t) \tag{A4}$$

where D is the diffusion coefficient.

The first step is to break up the total neutron flux into its prompt and delayed components

$$\phi = \phi^p + \phi^d \tag{A5}$$

Substitution of Equation A5 into equations A1 and A2 gives

$$\frac{1}{v}\frac{\partial\phi^p}{\partial t} = \left[(1-\beta_T)\,\chi_p\,\overline{P}-\overline{D}\right]\phi^p + S \tag{A6}$$

$$\frac{1}{v}\frac{\partial\phi^d}{\partial t} = \left[(1-\beta_T)\,\chi_p\,\overline{P}-\overline{D}\right]\phi^d + \sum_{i=1}^{M} i\,\lambda_i\,C_i \tag{A7}$$

$$\frac{\partial C_i}{\partial t} = \beta_i\,\overline{P}\,\phi^p + \beta_i\,\overline{P}\,\phi^d - \lambda_i\,C_i \tag{A8}$$

subject to the following constraints.

For convenience, the space, energy, and time dependencies are no longer explicitly noted. Equation A1 has been broken down into the separate Equations A6 and A7. This breakdown is permitted because of the nature of pulsed experiments. The extraneous source is only a short burst. After the burst, the resulting prompt neutrons decay quickly leaving only delayed neutrons. Note that Equation A7 describing the delayed-neutron flux includes prompt-neutron production from delayed-neutron absorption. These prompt neutrons are simply counted as additional delayed neutrons since their real-time behavior is determined by that of the delayed precursors.

Equations A5-A8 are satisfactory for thermal reactor systems but, as Gozani has noted, caution should be used in treating fast

reactor systems with such a physical model.[12]

The prompt and delayed-neutron fluxes are now defined in terms of shape functions and amplitude functions.

$$\phi^p(\vec{r},E,t) \equiv \Psi^p(\vec{r},E,t) \cdot T^p(t)$$
$$\text{and } \phi^d(\vec{r},E,t) \equiv \Psi^d(\vec{r},E,t) \cdot T^d(t) \tag{A9}$$

The shape functions, Ψ^p and Ψ^d, are explicitly dependent on space, energy and time. It is assumed, however, that the time dependences of the shape functions are relatively weak compared to those of the amplitude functions, T^p and T^d.

All the growth and subsequent decay of the total prompt- and delayed-neutron populations is to be contained in the amplitude functions, T^p and T^d. These amplitude functions are defined as

$$T^p(t) \equiv \int_o^\infty \int^{Vol} W(\vec{r},E) \frac{\phi^p(\vec{r},E,t)}{v(E)} \, dV \, dE$$
$$\text{and } T^d(t) \equiv \int_o^\infty \int^{Vol} W(\vec{r},E) \frac{\phi^d(\vec{r},E,t)}{v(E)} \, dV \, dE \tag{A10}$$

where $W(\vec{r},E)$ is some weighting function which may have dependence on space and energy, but not time. Clearly, if W were unity, T^p and T^d would be exactly the total number of prompt and delayed neutrons in the reactor at any given time. For other choices of W, T^p and T^d may be thought of as the integral of the weighted neutron densities over the reactor volume.

After substituting Equations A9 into Equations A10, it is found that W must have the useful properties that

$$\int_o^\infty \int_o^{Vol} W(\vec{r},E) \frac{\Psi^p(\vec{r},E,t)}{v(E)} \, dV \, dE = \langle W, v^{-1} \Psi^p \rangle$$
$$\int_o^\infty \int_o^{Vol} W(\vec{r},E) \frac{\Psi^d(\vec{r},E,t)}{v(E)} \, dV \, dE = \langle W, v^{-1} \Psi^d \rangle \tag{A11}$$

where bra-ket notation implies integration of the contained function convolutions over space and energy. Thus, the time derivatives of $\langle W, v^{-1} \Psi^p \rangle$ and $\langle W, v^{-1} \Psi^d \rangle$ must also be zero

The anticipated behavior of the shape functions may be explained in terms of the following analogy. The shape functions will change as a function of time in the same manner that water

in a bowl changes its distribution when the bowl is rocked. The distribution of water may change but the total amount of water does not. Similarly, ψ^p and ψ^d may change with time but $\langle W, v^{-1} \psi^p \rangle$ and $\langle W, v^{-1} \psi^d \rangle$ do not.

Substitute Equation A9 into Equations A6 and A7. Multiply the resulting equations by $W(\vec{r},E)$ and integrate over space and energy. Also substitute Equation A10 into Equation A8, but multiply by $W(\vec{r},E)\ \chi_i$ and integrate over all space and energy. The resulting equations, after noting the constancy of $\langle W, v^{-1} \psi^p \rangle$ and $\langle W, v^{-1}\psi^d \rangle$, are simply a re-expression of the "point reactor kinetics equations."

$$\frac{\partial T^p}{\partial t} = \left\langle W, \left[(1-\beta_T)\ \chi_p\ \overline{P}-\overline{D}\right] \psi^p \right\rangle T^p + \langle W, S \rangle \qquad \text{(A12)}$$

$$\frac{\partial T^d}{\partial t} = \left\langle W, \left[(1-\beta_T)\ \chi_p\ \overline{P}-\overline{D}\right] \psi^d \right\rangle T^d + \sum_{i=1}^{M} \langle W, \chi_i\ \lambda_i\ C_i \rangle \qquad \text{(A13)}$$

$$\frac{\partial}{\partial t} \langle W, \chi_i\ C_i \rangle = \langle W, \chi_i\ \beta_i\ \overline{P}\ \psi^p \rangle T^p + \langle W, \chi_i\ \beta_i\ \overline{P}\ \psi^d \rangle T^d - \langle W, \chi_i\ \lambda_i\ C_i \rangle \qquad \text{(A14)}$$

The usual pulsed-neutron experiment consists of repeatedly injecting short bursts of neutrons from the source into the reactor in a periodic fashion. Usually, the period, T_o, between bursts is sufficiently long that all the prompt neutrons from any single pulse decay before the next pulse. If the burst occurs at time t=0+, then

$$T^p(0) = T^p(T_o) = 0 \qquad \text{(A15)}$$

On the other hand, the delayed neutrons resulting from any single burst decay very slowly. As a result, delayed-neutron equilibrium is established at some time after pulsing begins. If delayed-neutron equilibrium has been established at time t=0, then

$$T^d(0) = T^d(T_o) \qquad \text{(A16)}$$

and

$$C_i(0) = C_i(T_o) \qquad \text{(A17)}$$

Integrate Equations A13 and A14 over one pulse period. (Equation A12 is no longer of any interest in this derivation.) The result is

$$0 = \int_o^{T_o} < W, \left[(1-\beta_T)\ \chi_p\ \overline{P}-\overline{D}\right]\ \psi^d > T^d\ dt$$

$$+ \int_o^{T_o} \sum_{i=1}^{M} < W, \chi_i\ \lambda_i\ C_i > dt \qquad \text{(A18)}$$

$$0 = \int_o^{T_o} < W, \chi_i\ \beta_i\ \overline{P}\ \psi^p > T^p\ dt$$

$$+ \int_o^{T_o} < W, \chi_i\ \beta_i\ \overline{P}\ \psi^d > T^d\ dt$$

$$- \int_o^{T_o} < W, \chi_i\ \lambda_i\ C_i > dt \qquad \text{(A19)}$$

Eliminate terms involving $<W, \chi_i\ \lambda_i\ C_i>$ between Equations A18 and A19. Also, use the definition of the total chi distribution

$$\chi_t \equiv \left[(1-\beta_T)\ \chi_p + \sum_{i=1}^{M} \chi_i\ \beta_i\right]$$

The result is

$$\sum_{i=1}^{M} \int_o^{T_o} <W, \chi_i\ \beta_i\ \overline{P}\ \psi^p>\ T^p\ dt = - \int_o^{T_o} <W, (\chi_T\ \overline{P}-\overline{D})\ \psi^d > T^d\ dt \qquad \text{(A20)}$$

We will now identify two quantities

$$\rho_A(t) \equiv \frac{<W, (\chi_T\ \overline{P}-\overline{D})\ \psi^d>}{<W, \chi_T\ \overline{P}\ \psi^d>} \qquad \text{(A21)}$$

and $$\beta_{eff_A}(t) \equiv \sum_{i=1}^{M} \frac{<W, \chi_i\ \beta_i\ \overline{P}\ \psi^p>}{<W, \chi_T\ \overline{P}\ \psi^p>} \qquad \text{(A22)}$$

If these definitions are substituted in Equation A20, we obtain

$$\int_o^{T_o} \beta_{eff_A}(t) \; \langle W, \chi_T \overline{P} \psi^p \rangle_{T^p} \, dt$$

$$= - \int_o^{T_o} \rho_A(t) \; \langle W, \chi_T \overline{P} \psi^d \rangle_{T^d} \, dt \qquad \text{(A23)}$$

All the time dependence of $\rho_A(t)$ is in ψ^d, which appears in both the numerator and denominator. In a repetitively pulsed, thermal lattice which has reached delayed-neutron equilibrium, $\phi^d(\vec{r},E,t)$ has only a weak dependence on time over the pulse period. Since ψ^d, having an even weaker dependence on time, appears in both the numerator and denominator of $\rho_A(t)$, whatever time dependence there is in both numerator and denominator must very nearly cancel. Thus, it is reasonable to treat $\rho_A(t)$ as independent of time and factor it out of the time integral.

Similarly, we can show that $\beta_{eff_A}(t)$ is to a good approximation independent of time. Therefore,

$$-\frac{\rho_A}{\beta_{eff_A}} = \frac{\int_o^{T_o} \langle W, \chi_T \overline{P} \psi^p \rangle_{T^p} \, dt}{\int_o^{T_o} \langle W, \chi_T \overline{P} \psi^d \rangle_{T^d} \, dt}$$

$$= \frac{\int_o^{T_o} \langle W, \chi_T \overline{P} \phi^p \rangle \, dt}{\int_o^{T_o} \langle W, \chi_T \overline{P} \phi^d \rangle \, dt} \qquad \text{(A24)}$$

Equation A24 is the Generalized Area Method equation.

The Generalized Area equation also appears in the work of Becker and Quisenberry (Reference 13, Equation 43); however, that equation was derived under the assumption that both ψ^p and ψ^d were independent of time. Figures 2-4 clearly show that this is a very poor assumption. Also, no use of the equation was suggested by Becker and Quisenberry as a means of determining the subcritical reactivity from data collected with distributed neutron detectors.

Kosály and Fischer[8] also derived the Generalized Area equation, but under the assumption that the prompt and delayed fluxes were expanded in terms of the kinetic eigenfunction set

$$\phi^p(\vec{r},E,t) \equiv \sum_{i=1}^{\infty} \psi_i^p(\vec{r},E) \, T_i \, e^{\alpha_i t}$$

$$\text{and } \phi^d(\vec{r},E,t) \equiv \sum_{i=1}^{\infty} \psi_i^p(\vec{r},E)\, T_i\, e^{\alpha_i t}$$

Here, the ψ_i^p and ψ_i^d are the modal shape functions for the prompt and delayed neutrons respectively. Thus, the objection to Becker and Quisenberry's use of a totally time independent shape function was removed. However, the Kosály-Fischer derivation leads to the Generalized Area Equation with only $W = \phi_s^+$ weighting. Nevertheless, they do give numerical examples of data from several distributed detectors where both unit weighting and static adjoint weighting are used to find the subcritical reactivity according to the Generalized Area equation. The results are in agreement with the conclusions of this report.

B. Approximations to the Generalized Area Method

In Becker and Quisenberry's development, the shape functions ψ^p and ψ^d are assumed to be time independent.[13] If ψ^p and ψ^d are assumed independent of time, then Equation A24 becomes

$$\frac{\rho_A}{\beta_{eff_A}} = -\frac{\langle W,\ \chi_T\ \overline{P}\ \psi_o^p \rangle \int_o^{T_o} T^p\, dt}{\langle W,\ \chi_T\ \overline{P}\ \psi_o^d \rangle \int_o^{T_o} T^d\, dt} \tag{B1}$$

Becker and Quisenberry identify a normalization constant

$$N_c \equiv \frac{\langle W,\ \chi_T \overline{P}\ \psi_o^p \rangle}{\langle W,\ \chi_T P\ \psi_o^d \rangle}$$

Thus

$$\frac{\rho_{BQ}}{\beta_{eff_{BQ}} N_c} \cong -\frac{\int_o^{T_o} T^p\, dt}{\int_o^{T_o} T^d\, dt} = -\frac{\psi_o^d}{\psi_o^p} \frac{\int_o^{T_o} \phi^p\, dt}{\int_o^{T_o} \phi^d\, dt} \tag{B2}$$

This is called the Becker-Quisenberry approximation for single detector analysis.

The development of the even simpler Sjöstrand approximation requires only the identification that $\psi_o^p = \psi_o^d$.[1] Then

$N_c = 1$ and

$$\frac{\rho_{Sjö}}{\beta_{eff_{Sjö}}} \cong - \frac{\int_o^{T_o} \phi^p \, dt}{\int_o^{T_o} \phi^d \, dt} \tag{B3}$$

Clearly, the Sjöstrand approximation is strictly valid only for a homogeneous lattice which is very small so that higher order harmonics are not excited appreciably.

C. Derivation of the Prompt Neutron Eigenequation

The following derivation of the prompt neutron eigenequation follows Preskitt's treatment.[4] Preskitt also starts with the basic diffusion theory (Equations A1 and A2). However, he immediately expands the total neutron flux and precursor concentrations into a series of harmonic terms in which the shape functions are explicitly time independent.

$$\phi(\vec{r},E,t) = \sum_{n=1}^{\infty} \psi_n(\vec{r},E) \, e^{\alpha_n t}$$

$$\text{and } C_i(\vec{r},t) = \sum_{n=1}^{\infty} C_{ni}(\vec{r}) \, e^{\alpha_n t} \tag{C1}$$

Substitute Equations C1 in A1 and A2; restrict attention to time after completion of the source burst; and eliminate C_{ni}. The result is

$$0 = \left[\left(\frac{-\alpha_n}{v} - \overline{D} \right) + (1-\beta_T)\chi_p \overline{P} + \sum_{i=1}^{M} \chi_i \lambda_i \frac{\beta_i \overline{P}}{(\lambda_i + \alpha_n)} \right] \psi_n \tag{C2}$$

A quantity χ_k is defined as

$$\chi_k \equiv (1-\beta_T)\chi_p + \sum_{i=1}^{M} \chi_i \lambda_i \frac{B_i}{(\lambda_i + \alpha_n)}$$

and called the kinetic spectrum operator. Equations A1 and A2 have evolved to the much simpler form

$$0 = \left[\left(\frac{-\alpha_n}{v} - \overline{D} \right) + \chi_k \overline{P} \right] \psi_n \tag{C3}$$

The pulsed neutron experiment has two very distinct time domains. Just after the source burst, the prompt neutrons are far more numerous than the delayed neutrons. Thus, $\phi \cong \phi^p$ in most of the prompt decay region. All the prompt mode decay constants are very much larger than any of the λ_i values, the precursor decay constants. Thus, in the prompt region

$$\chi_k \cong (1-\beta_T)\chi_p$$

and the time eigenequation for the prompt neutrons is approximated by

$$0 = \left[\left(\frac{-\alpha_n}{v} - \overline{D}\right) + (1-\beta_T)\chi_p\overline{P}\right]\psi_n^p \qquad (C4)$$

The other time domain of importance is the delayed neutron region where $\phi \cong \phi^d$. In this region, the flux is decaying very slowly, at rates similar to the precursor decay constants λ_i. Thus, the delayed modes must have decay constants that cluster about the λ_i values; therefore, $\alpha_n/v << \overline{D}$ in the delayed region. The delayed eigenequation is approximated well by

$$0 = (-\overline{D} + \chi_k\overline{P})\ \psi_n^d$$

But in the limit that α_n is very small, the kinetic spectrum operator approaches the total fission spectrum operator defined by

$$\chi_T \equiv (1-\beta_T)\ \chi_p + \sum_{i=1}^{M} \chi_i\beta_i$$

Thus,

$$0 = (-\overline{D} + \chi_T\overline{P})\ \psi_n^d \qquad (C5)$$

Equation C5 is the source of the often made assertion that the delayed neutron, harmonic eigenfunctions are very similar to the static harmonic eigenfunctions. This is true because static codes solve

$$0 = \left(-\overline{D} + \frac{\chi_T\overline{P}}{k_{eff}}\right)\ \phi_s$$

where k_{eff} is the scale factor which assures neutron balance.

Clearly, however, $\psi_n^p \neq \psi_n^d$ in reflected reactors even for the fundamental mode. The non-equivalence of the prompt and delayed harmonic eigenfunctions gives rise to the phrase "kinetic distortion."

REFERENCES

1. N. G. Sjöstrand. "Measurements on a Subcritical Reactor Using a Pulsed Neutron Source." *Arkiv Für Fysik 11*, 233 (1956).

2. E. Garelis and J. L. Russell, Jr. "Theory of Pulsed Neutron Source Measurements." *Nucl. Sci. Eng.* 16, 263 (1963).

3. T. Gozani. *The Theory of the Modified Pulsed Source Technique. Report EIR-Bericht 79*, Würenlingen Institut, Switzerland (1965).

4. C. A. Preskitt, E. A. Nephew, J. R. Brown, and K. R. VanHowe. "Interpretation of Pulsed-Source Experiments in the Peach Bottom HTGR." *Nucl. Sci. Eng. 29*, 283 (1967).

5. G. Kosály, J. Valkó, and A. Fischer. "Theory of the Area Ratio Method of Subcriticality Determination." *Atomkernenergie 23*, 251 (1974).

6. P. B. Parks. *Methods of Analysis to Determine Subcritical Reactivity from the Pulsed Neutron Experiment.* USAEC Report DP-1367, E. I. du Pont de Nemours and Co., Savannah River Laboratory, Aiken, SC (1975).

7. G. E. Bell and S. Glasstone. *Nuclear Reactor Theory*, p. 546, Van Nostrand Reinhold Co., New York (1971).

8. G. Kosály and A. Fischer. "On Integral-Versions of the Area-Ratio Method of Pulsed Neutron Reactivity Measurements." *J. Nucl. Energy 26*, 17 (1972).

9. M. E. Radd. *WIGLE-40, A Two-Group, Time Dependent Diffusion Theory Program for the IBM 7040 Computer.* USAEC Report IDO-17125, Phillips Petroleum Co., Idaho Falls, Idaho (1965).

10. A. F. Henry. *Nuclear Reactor Analysis* (Chapter 7), The MIT Press, Cambridge, Massachusetts (1975).

11. J. Dorning. "Determination of Reactivity by the Pulsed Source Method when Die-Away Is Not Purely Exponential." *Trans. Am. Nucl. Soc. 15*, 904 (1972).

12. T. Gozani. "Consistent Subcritical Fast-Reactor Kinetics." p. 109 *Dynamics of Nuclear Systems.* D. L. Hetrick, ed., University of Arizona Press, Tucson, Arizona (1972).

13. M. Becker and K. S. Quisenberry. "The Spatial Dependence of Pulsed Neutron Reactivity Measurements." *Symposium of Neutron Dynamics and Control at the University of Arizona*, Tucson, Arizona, April (1965). CONF-650406-2.